Acta Crystallographica Section D
Biological Crystallography
ISSN 0907-4449

The 2C putative helicase of echovirus 30 adopts a hexameric ring-shaped structure

Nicolas Papageorgiou,[a] Bruno Coutard,[a] Violaine Lantez,[a] Eric Gautron,[b] Olivier Chauvet,[b] Cécile Baronti,[c] Heléne Norder,[d] Xavier de Lamballerie,[c] Vasile Heresanu,[e] Nathalie Ferté,[e] Stéphane Veesler,[e] Alexander E. Gorbalenya[f] and Bruno Canard[a]*

[a]Architecture et Fonction des Macromolécules Biologiques, UMR 6098 Centre National de la Recherche Scientifique, Université de la Méditerranée and Université de Provence, Case 925, 163 Avenue de Luminy, 13288 Marseille CEDEX 9, France, [b]Institut des Matériaux Jean Rouxel, IMN UMR 6502, Université de Nantes, 2 Rue de la Houssinière BP 32229, 44322 Nantes CEDEX 3, France, [c]Unité des Virus Emergents, UMR 190 'Emergence des Pathologies Virales', Université de la Méditerranée et Institut de Recherche pour le Développement, Marseille, France, [d]Department of Virology, Swedish Institute for Infectious Disease Control, 171 82 Solna, Sweden, [e]CINaM–CNRS, Campus de Luminy, Case 913, 13288 Marseille CEDEX 9, France, and [f]Molecular Virology Laboratory, Department of Medical Microbiology, Center of Infectious Diseases, Leiden University Medical Center, LUMC P4-26, PO Box 9600, 2300 RC Leiden, The Netherlands

Correspondence e-mail: bruno.canard@afmb.univ-mrs.fr

Received 3 March 2010
Accepted 14 July 2010

The 2C protein, which is an essential ATPase and one of the most conserved proteins across the *Picornaviridae* family, is an emerging antiviral target for which structural and functional characterization remain elusive. Based on a distant relationship to helicases of small DNA viruses, piconavirus 2C proteins have been predicted to unwind double-stranded RNAs. Here, a terminally extended variant of the 2C protein from echovirus 30 has been studied by means of enzymatic activity assays, transmission electron microscopy, atomic force microscopy and dynamic light scattering. The transmission electron-microscopy technique showed the existence of ring-shaped particles with ∼12 nm external diameter. Image analysis revealed that these particles were hexameric and resembled those formed by superfamily 3 DNA virus helicases.

1. Introduction

The large *Picornaviridae* family comprises non-enveloped viruses with a single positive-stranded RNA genome (Semler & Wimmer, 2002; Racaniello, 2007). The genome is translated by a cap-independent mechanism to produce a polyprotein that is autoproteolytically processed to structural proteins, which form virions, and nonstructural proteins, which mediate the virus life cycle. Three highly conserved nonstructural proteins with enzymatic activity, the 2C ATPase, the 3C protease and the 3D RNA-dependent RNA polymerase, control different steps in virus replication and constitute attractive targets for antiviral therapy. The 2C protein (330 amino acids) is a putative helicase that was predicted to include three domains (Tolskaya *et al.*, 1994), with the highly conserved ATPase domain (Gorbalenya *et al.*, 1990; Mirzayan & Wimmer, 1994; Klein *et al.*, 1999; Rodriguez & Carrasco, 1993; Pfister *et al.*, 2000; Samuilova *et al.*, 2006) being flanked by two domains with RNA-binding activity (Rodriguez & Carrasco, 1995). Helicases unwind double-stranded DNA or RNA in reactions fuelled by ATP hydrolysis (Tuteja & Tuteja, 2004*a*,*b*). Based on characteristic sequence conservation of critically important residues, several superfamilies/families of helicases have been identified (SF1–3; Gorbalenya & Koonin, 1993). The 2C proteins of picornaviruses and related proteins in other RNA viruses belong to the so-called helicase superfamily 3 (SF3). Picornavirus helicases have no significant sequence similarity to any other viral helicases from the other helicase superfamilies, except for very short sequence stretches in an NTP-binding/hydrolysis site. Because helicases generally need energy to unwind their nucleic acid substrates, the NTP-binding/hydrolysis site is a part of the helicase signature sequence. In the picornavirus 2C proteins, the helicase signature includes three conserved sequence motifs: the ubiquitous Walker A and B motifs mediating ATP binding (Walker *et al.*, 1982) and the SF3-specific motif C (Gorbalenya *et al.*, 1990; Guenther *et al.*, 1997). SF3 also includes proven helicases encoded by small DNA viruses which adopt a characteristic ring-shaped structure formed by six monomers as described for the simian virus 40 large T antigen (SV40 LTag; Li *et al.*, 2003), the replication protein of adeno-associated virus type 2 (AAV2 Rep40; James *et al.*, 2003, 2004) and the replication protein E1 of human papillomavirus serotype 18 (HPV18 RepE1; Abbate *et al.*, 2004). Previous studies succeeded in expressing and purifying the 2C protein carrying a large soluble N-terminal tag

such as MBP (Rodriguez & Carrasco, 1993) or GST (Klein *et al.*, 1999; Pfister *et al.*, 2000) or with no tag at all (Klein *et al.*, 1999). Recently, the poliovirus 2C domain in fusion with MBP was shown to be organized as pentamers to octamers (Adams *et al.*, 2009), while negative-stain electron microscopy of foot and mouth disease virus (FMDV) 2C–ATP–RNA complexes revealed hexameric ring structures (Sweeney *et al.*, 2010).

Here, we report the study of a terminally extended variant of the 2C protein derived from echovirus 30 (EV-30) by means of enzymatic activity assays, transmission electron microscopy (TEM), atomic force microscopy (AFM) and dynamic light scattering (DLS). Using TEM we show that among several other oligomerizations, the protein adopts a hexameric ring-shaped structure which resembles the hexameric organization of DNA virus helicases belonging to SF3.

2. Materials and methods

2.1. Protein expression and purification

The EV-30 cDNA (strain 548-00-SE-M-E-30, isolated from the stools of a patient with aseptic meningitis) was amplified and characterized from viral RNA as described previously (Emonet *et al.*, 2007). One construct encompassed the entire 2C locus (329 amino acids), while 15 other constructs encompassed the entire 2C locus with variable extensions into the neighbouring 2B and/or 3A loci with increments of five, ten and 15 amino acids (Fig. 1*a*). A sequence coding for a six-histidine tag was introduced at the 5′-end of the PCR product inserted by recombination in pDEST14 using the Gateway cloning protocol (Invitrogen). The expression plasmid was then transformed in Rosetta pLysS *Escherichia coli* cells (Novagen) for expression. Cells were grown in 2YT medium containing 100 µg ml^{-1} ampicillin and 34 µg ml^{-1} chloramphenicol at 310 K. Protein expression was induced overnight at 290 K with 0.5 m*M* isopropyl *β*-D-1-thiogalactopyranoside (IPTG). The cells were harvested by centrifugation and resuspended in 50 ml lysis buffer (50 m*M* Tris, 300 m*M* NaCl, 10 m*M* imidazole, 5% glycerol, 0.1% Triton, 2 m*M* EDTA pH 8) complemented with 0.25 mg l^{-1} lysozyme, Complete EDTA-free protease-inhibitor cocktail (Roche), 10 µg ml^{-1} DNase I and 20 m*M* $MgSO_4$. The bacterial sample was sonicated and centrifuged at 25 000*g* for 30 min. The recombinant protein was purified from the supernatant by immobilized metal-affinity chromatography (IMAC) on a HisPrep column (GE Healthcare) and eluted with a buffer consisting of 50 m*M* Tris, 300 m*M* NaCl, 500 m*M* imidazole pH 8. The eluted protein was purified by size-exclusion chromatography (SEC) on a HiLoad 16/60 Superdex 200 column (GE Healthcare) in 10 m*M* Tris, 300 m*M* NaCl, 2 m*M* DTT pH 7.5. The main SEC peak was collected and assessed for purity by SDS–PAGE (Fig. 1*c*). Finally, the protein was concentrated to 2 mg ml^{-1} for enzymatic assays.

2.2. ATPase and helicase assays

ATPase reactions (50 µl) were performed in triplicate at 310 K in the reaction buffer (50 m*M* Tris–HCl pH 7.5, 100 m*M* NaCl, 10 m*M* $MgCl_2$ and 0.1 mg ml^{-1} BSA) described previously for the 2C protein of coxsackie B3 virus (De Palma *et al.*, 2008). Reactions were stopped by the addition of 2.5 µl 0.5 *M* EDTA. 20 µl aliquots of the reaction mixture were withdrawn over time to measure the released inorganic phosphate concentration using a previously described colorimetric assay (Gawronski & Benson, 2004). The Henri–Michaelis–Menten equation was used to determine V_m and K_m for the the ATPase

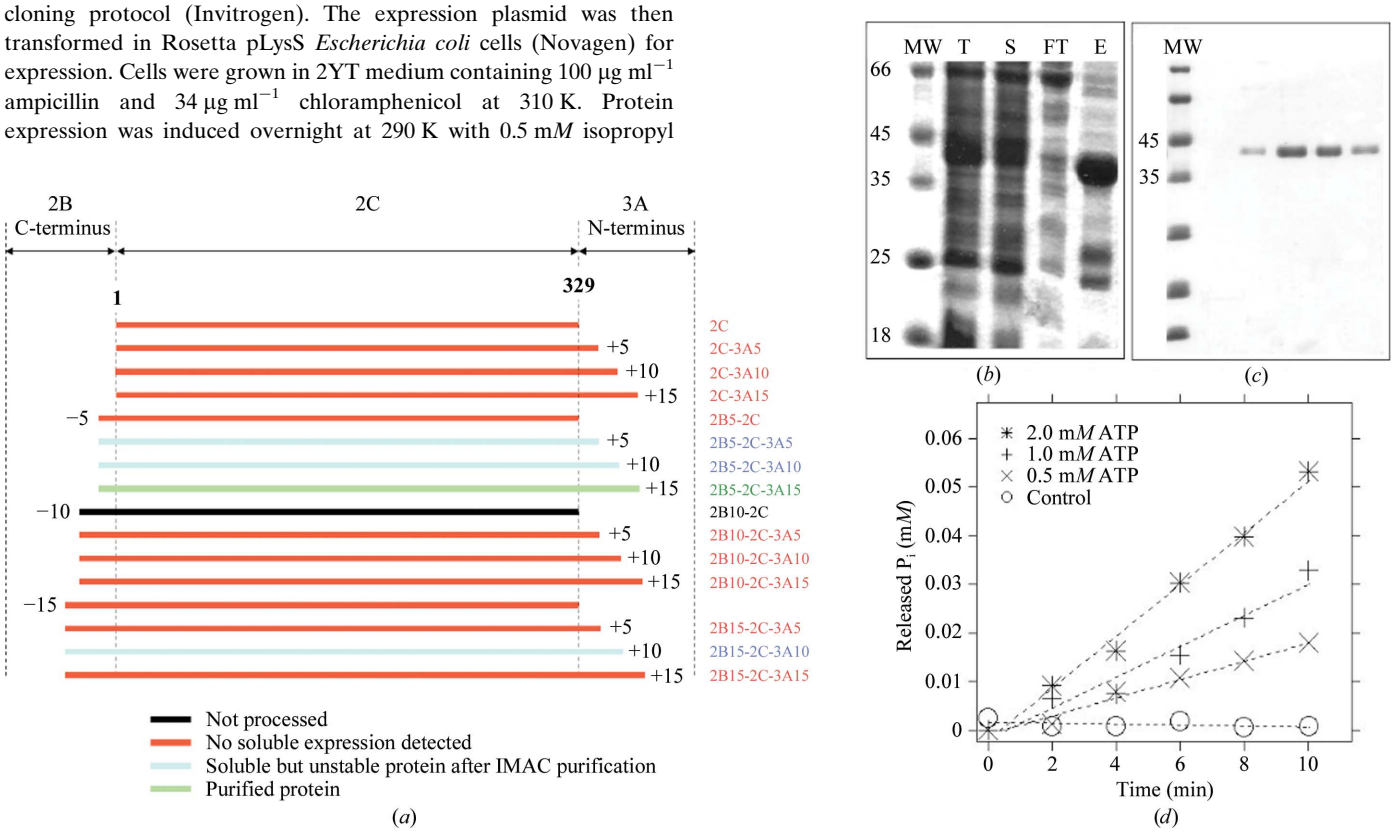

Figure 1
Purification of EV-30 2B5-2C-3A15 and ATPase activity. (*a*) Schematic drawing of 16 investigated clones containing 2C. The corresponding names shown on the right side of the diagram indicate the sizes of the peptides from 2B and/or 3A fused to 2C in a given construct. (*b*) Purification of EV-30 2B5-2C-3A15. Coomassie Blue-stained SDS–PAGE gel of the fractions collected during the IMAC purification: MW, molecular-weight markers (labelled in kDa); T, total expression; S, soluble fraction; FT, flowthrough; E, elution. (*c*) Collected fractions after gel filtration. (*d*) ATPase activity of EV-30 2B5-2C-3A15 at various ATP concentrations monitored by the release of inorganic phosphate in the time-course experiment aiming to define V_i. The Japanese encephalitis virus 2′-*O*-methyltransferase domain purified under the same conditions as EV-30 2B5-2C-3A15 was used as a negative control for ATPase activity (open circles)

activity. Assays at different protein concentrations as well as the time course of the ATP hydrolysis revealed a specific phosphohydrolase activity for which V_i could be defined at several ATP concentrations (Fig. 1*d*). RNA and DNA unwinding was assessed following a previously described protocol (Speroni *et al.*, 2008).

2.3. DLS, AFM and TEM

DLS measurements were carried out using a Sematech SEM 633 light-scattering apparatus (Sematech, Nice, France) and a Spectra Physics 2017 5 W argon-ion laser running at a power ranging from 50 to 500 mW, operating at 514 nm and processed through an RTG correlator (Sematech, Nice, France). Prior to measurements, the samples were filtered through a 0.5 µm Millex LCR single-use membrane (Millipore) before being transferred into a 12 mm diameter cylindrical glass cuvette with a flat bottom. The analysis volume was about 300 µl for a protein concentration of 1 mg ml^{-1}.

AFM measurements were performed with a Digital Nanoscope III atomic force microscope equipped with a 12 µm scanner. Images were collected with a typical scan rate of 1 Hz in the tapping mode using oxide-sharpened Si_3N_4 cantilever tips (Nanoprobe). The protein at concentrations ranging from 0.05 to 0.1 mg ml^{-1} was adsorbed on glass plates previously chemically etched with NaOH solution at 1 *M* for 1 min. TEM measurements were performed with a 300 keV Hitachi HNAR 9000 electron microscope at a 50 000 magnification. The purified protein at a concentration of 0.05 mg ml^{-1} was adsorbed on carbon-coated copper grids that had previously been charged in glow discharge and stained with 2% ammonium molybdate. 1.5 µm^2 grid regions were photographed onto Kodak film (Electron SO-163) and scanned with a raster step of 2400 dpi (10.6 µm) at a resolution of 2.1 Å per pixel. The scanned images were converted to eight-bit TIFF files for subsequent processing by the *EMAN* v.1.9 program suite (Ludtke *et al.*, 1999). The particles were picked manually using the *BOXER* routine; correction of the transfer function (CTF) was performed with the

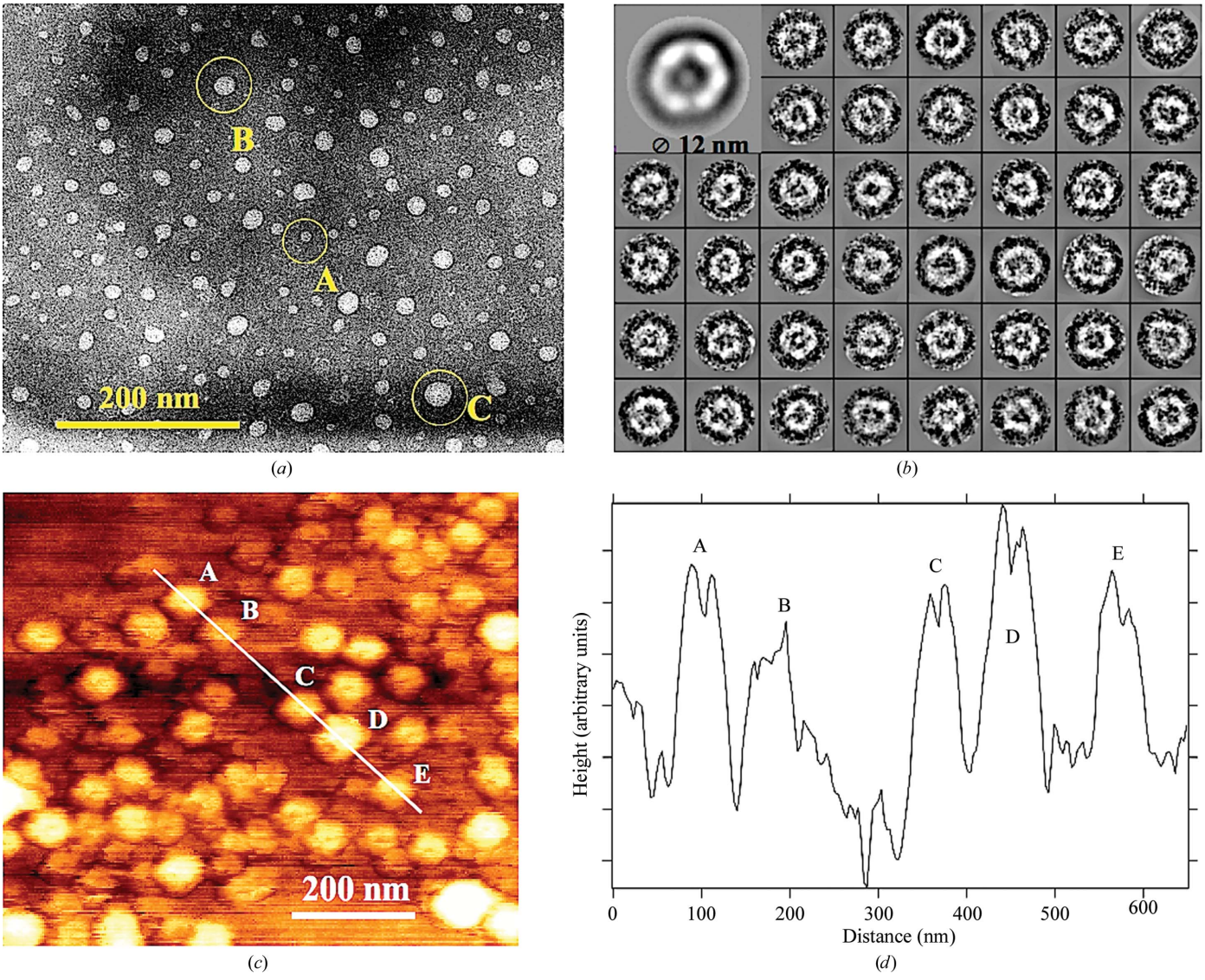

Figure 2
(*a*) Typical TEM image (600 × 500 nm, 300 keV, ×50 000) of small and intermediate-sized particles; the particles labelled A, B and C have diameters of 10, 30 and 40 nm, respectively. (*b*) Ring-shaped particles with a typical external diameter of 12 nm. The upper right inset of the figure shows an average image of these particles calculated with no symmetry constraints imposed, showing evidence of hexameric organization. (*c*) 900 × 900 nm AFM image of particles with dimensions ranging from 40 to 100 nm. (*d*) Measured horizontal dimension for the particles labelled A–E along the white line shown in Fig. 2(*c*).

CTFIT routine, while alignment and averaging of the particle images were performed with the *CLASSALIGN*2 routine.

3. Results and discussion

Of the 16 EV30 2C protein constructs (Fig. 1*a*) only four, 2B5-2C-3A5, 2B5-2C-3A10, 2B5-2C-3A15 and 2B15-2C-3A10, yielded soluble protein. Finally, only the 2B5-2C-3A15 protein (referred to as 2C in the following for simplicity) remained stable in solution after IMAC (Fig. 1*b*). During SEC the protein eluted as a heterogeneous population which was assessed for ATPase and helicase activity. For the ATPase activity we found a $V_{\rm m}$ value of 5.8 ± 0.9 μM min^{-1} and a $K_{\rm m}$ value of 0.81 ± 0.18 mM, which were similar to those previously reported for poliovirus 2C (Pfister *et al.*, 2000). Likewise, no helicase activity was detected on either DNA or RNA substrates.

The TEM, AFM and DLS techniques showed a high heterogeneity of the samples and in particular the presence of large aggregates. Quantitative characterization of the samples by means of DLS turned out to be impossible owing to the fact that the scattered intensity (which is proportional to the square of the mass) from large heavy particles masked the contribution of lighter oligomers. TEM and AFM measurements confirmed that the largest amount of the protein forms aggregates with dimensions ranging from 10 to 200 nm. The same aggregation trend was observed for samples processed by TEM or AFM either immediately after purification as well as after 1–2 weeks of storage at 277 K. Fig. 2(*a*) illustrates a typical TEM image of small and intermediate-sized particles such as the particles labelled A, B and C, which present diameters of 10, 30 and 40 nm, respectively. Fig. 2(*c*) demonstrates an AFM image of a population of particles with dimensions ranging from 40 to 100 nm. Fig. 2(*d*) shows the measured dimensions for the particles labelled A–E along the white line shown in Fig. 2(*c*). Larger aggregates with dimensions up to 200 nm were also observed with both the AFM and TEM techniques.

Among the particles observed by TEM, we were able to isolate repeatedly observed ring-shaped particles with an external diameter of 12 ± 1 nm and an inner diameter of 4 ± 0.5 nm such as those presented in Fig. 2(*b*). The ring-shaped particle yield was significantly higher in the presence of ADP. Indeed, two sets of samples (30 TEM photographs each) either exposed or not exposed to 3 mM ADP were studied by TEM. We collected 1200 particles for the former and 180 particles for the latter. The particles considered in the following discussion correspond to the samples exposed to 3 mM ADP.

The upper left inset of Fig. 2(*b*) illustrates an average image of the observed ring-shaped particles calculated with no symmetry constraints imposed. The average image was calculated as follows. The particle images were first aligned to a common reference. Averaging of the aligned images generated a new reference that was used for a new iteration of alignment. Each iteration generates a class average that is more consistent with the data. After each iteration, each aligned image is compared with the class average from the previous iteration. If the quality of the match is worse than a certain threshold value the image is discarded. The average image shown in Fig. 2(*b*) was calculated after eight iterations using a threshold of one standard deviation. According to this method 288 images of the 1200 initially collected were discarded, while the remaining 912 match the average image (mean value) within one standard deviation. The average image shows a hexameric organization. We stress that the observed hexamer particles represent only a minority of the deposited molecules, while their relative fraction may not be reliably estimated without knowing the grid retention constants for aggregates, monomers and oligomers. A precise quantification of the ratio of hexamer particles in the absence and in the presence of ADP was not possible by SEC as these particles remained rare in both cases. However, a rough estimation of the relative quantity of these hexamer particles can be deduced from SEC, in which a broad mass distribution was detected between 200 and 500 kDa. The latter has been numerically fitted considering four Gaussian functions of the same linewidth corresponding to sixfold, eightfold, ninefold and tenfold oligomers. According to this fit, hexamers may represent less than 2% of the total oligomer population.

4. Conclusions

In conclusion, we have studied an extended derivative of EV-30 2C which was found to be active as an ATPase but inactive as a helicase. DLS as well as SEC measurements showed a high tendency to aggregation, but failed to quantitatively characterize the state of the samples. In contrast, TEM and AFM measurements were able to distinguish aggregated particles with dimensions ranging from 10 to 200 nm. TEM images revealed that among other oligomeric forms the protein can adopt a hexameric form reminiscent of that of distantly related viral DNA helicases belonging to SF3, such as SV40 LTag (Li *et al.*, 2003), AAV2 Rep40 (James *et al.*, 2003, 2004) and HPV18 RepE1 (Abbate *et al.*, 2004).

We thank Armando De Palma and Johan Neyts for sharing valuable information concerning the 2C protein. Part of this work was carried out using the resources of the Computational Biology Service Unit from Cornell University, which is partially funded by the Microsoft Corporation. This work was supported in part by the VIZIER integrated project (LSHG-CT-2004-511960) of the European Union Sixth Framework Programme (FP6) and the funding program 'Maladies Infectieuses Emergentes' from the French Ministry of Research.

References

Abbate, E. A., Berger, J. M. & Botchan, M. R. (2004). *Genes Dev.* **18**, 1981–1996.
Adams, P., Kandiah, E., Effantin, G., Steven, A. C. & Ehrenfeld, E. (2009). *J. Biol. Chem.* **284**, 22012–22021.
De Palma, A. M., Vliegen, I., De Clercq, E. & Neyts, J. (2008). *Med. Res. Rev.* **28**, 823–884.
Emonet, S. F., Grard, G., Brisbarre, N. M., Moureau, G. N., Temmam, S., Charrel, R. N. & de Lamballerie, X. (2007). *Nature Protocols*, **2**, 340–346.
Gawronski, J. D. & Benson, D. R. (2004). *Anal Biochem.* **327**, 114–118.
Gorbalenya, A. E. & Koonin, E. V. (1993). *Curr. Opin. Struct. Biol.* **3**, 419–429.
Gorbalenya, A. E., Koonin, E. V. & Wolf, Y. I. (1990). *FEBS Lett.* **262**, 145–148.
Guenther, B., Onrust, R., Sali, A., O'Donnell, M. & Kuriyan, J. (1997). *Cell*, **91**, 335–345.
James, J. A., Aggarwal, A. K., Linden, R. M. & Escalante, C. R. (2004). *Proc. Natl Acad. Sci. USA*, **101**, 12455–12460.
James, J. A., Escalante, C. R., Yoon-Robarts, M., Edwards, T. A., Linden, R. M. & Aggarwal, A. K. (2003). *Structure*, **11**, 1025–1035.
Klein, M., Eggers, H. J. & Nelsen-Salz, B. (1999). *Virus Res.* **65**, 155–160.
Li, D., Zhao, R., Lilyestrom, W., Gai, D., Zhang, R., DeCaprio, J. A., Fanning, E., Jochimiak, A., Szakonyi, G. & Chen, X. S. (2003). *Nature (London)*, **423**, 512–518.
Ludtke, S. J., Baldwin, P. R. & Chiu, W. (1999). *J. Struct. Biol.* **128**, 82–97.
Mirzayan, C. & Wimmer, E. (1994). *Virology*, **199**, 176–187.
Pfister, T., Jones, K. W. & Wimmer, E. (2000). *J. Virol.* **74**, 334–343.
Racaniello, V. (2007). *Fields Virology*, edited by D. Knipe, P. M. Howley, D. E. Griffin, R. A. Lamb, M. A. Martin, B. Roizman & S. E. Straus, Vol. 1, pp. 795–838. Philadelphia: Wolters Kluwer/Lippincott, Williams & Wilkins.
Rodriguez, P. L. & Carrasco, L. (1993). *J. Biol. Chem.* **268**, 8105–8110.
Rodriguez, P. L. & Carrasco, L. (1995). *J. Biol. Chem.* **270**, 10105–10112.
Samuilova, O., Krogerus, C., Fabrichniy, I. & Hyypiä, T. (2006). *J. Virol.* **80**, 1053–1058.
Semler, B. L. & Wimmer, E. A. F. (2002). Editors. *Molecular Biology of Picornaviruses*, p. 502. Washington: ASM Press.

Speroni, S., De Colibus, L., Mastrangelo, E., Gould, E., Coutard, B., Forrester, N. L., Blanc, S., Canard, B. & Mattevi, A. (2008). *Proteins*, **70**, 1120–1123.
Sweeney, T. R., Cisnetto, V., Bose, D., Bailey, M., Wilson, J. R., Zhang, X., Belsham, G. J. & Curry, S. (2010). *J. Biol. Chem.* **285**, 24347–24359.
Tolskaya, E. A., Romanova, L. I., Kolesnikova, M. S., Gmyl, A. P., Gorbalenya, A. E. & Agol, V. I. (1994). *J. Mol. Biol.* **236**, 1310–1323.
Tuteja, N. & Tuteja, R. (2004*a*). *Eur. J. Biochem.* **271**, 1835–1848.
Tuteja, N. & Tuteja, R. (2004*b*). *Eur. J. Biochem.* **271**, 1849–1863.
Walker, J. E., Saraste, M. Runswick, M. J. & Gay, N. J. (1982). *EMBO J.* **1**, 945–951.